Studies of 4 lepton final states of ttZ production in pp collisions with the CMS experiment at $\sqrt{s} = 8$ TeV

Abigail O'Rourke, University of Manchester, UK

September 4, 2013

Supervised by Johannes Hauk and Andreas B. Meyer

Abstract

A study is made of ttZ production in 4 lepton final states at the CMS experiment at $\sqrt{s} = 8\,\mathrm{TeV}$ and $\int \mathcal{L}\mathrm{dt} = 19.8\,\mathrm{fb}^{-1}$. This analysis aims to optimise the event selection steps by studying lepton and jet requirements. A measurement of the cross section of the ttZ process is made with the final event selection requirements, and determined to be $\sigma_{\mathrm{inc}}^{\mathrm{ttZ}} = 191 \pm 143\,\mathrm{fb}$. The measurement is strongly limited by the statistical precision but shows agreement with the theoretical prediction of $\sigma_{\mathrm{inc}}^{\mathrm{ttZ}} = 206\,\mathrm{fb}$.

Contents

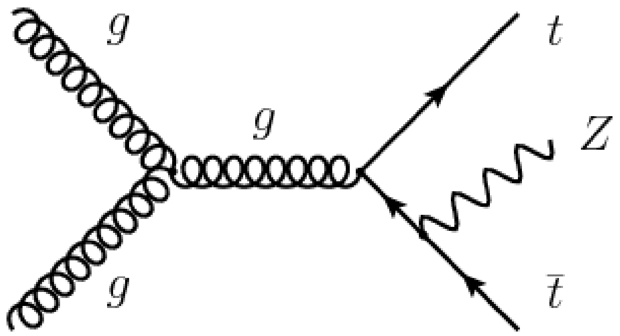

Figure 1: A leading order Feynman diagram of the $t\bar{t}Z^0$ process investigated in this analysis.

1 Introduction

This note presents a study conducted at the DESY summer student program of $t\bar{t}Z^0$ production in 4 lepton final states observed with pp collisions at the CMS experiment [1] at $\sqrt{s} = 8\,\text{TeV}$ using data collected in 2012 with an integrated luminosity of $\int \mathcal{L}dt = 19.8\,\text{fb}^{-1}$. This refers to $t\bar{t}$ events where each (anti-)top quark decays to leptons via $W^{\pm}$ and one (anti-)bottom quark, where an additional Z^0 boson is radiated which also decays leptonically. The Z^0 boson is identified by an opposite sign same flavour lepton pair within the Z^0 mass range. The process can be further separated from backgrounds by requiring the presence of identified bjets.

The relevance of the study of this process is a test of the Standard Model by comparing experimental data with theoretical predictions. A measurement of this process at $\sqrt{s} = 7\,\text{TeV}$ exists [2], and these results are in agreement with the SM within the uncertainty, although the data was underestimated by the prediction [3]. However this study uses different final state selection requirements, aiming for 3 lepton processes. Another motivation for studying this process is that it is also a background in all rare multilepton processes. Additionally, $t\bar{t}Z^0$ with $Z^0 \rightarrow b\bar{b}$ is a relevant background for $t\bar{t}H$ searches, with the similar masses of the bosons. Observing $t\bar{t}Z^0$ in a clean signal to background ratio could provide insight into the $t\bar{t}Z^0$ ($Z^0 \rightarrow b\bar{b}$) process.

Simulated data samples are compared to data samples recorded at the CMS detector in 2012. The simulation signal used is $t\bar{t}Z^0$. The main background contributions are the ZZ to 4l, $t\bar{t}W^+W^-$, ZZZ and WWZ processes. A simulation of the $t\bar{t}H$ process is included as the analysis could possibly be sensitive to this process, and additional information might be provided about the process. The simulated data samples are subject to the same requirements in the analysis and are used for comparisons of the theoretical predictions with the data.

This note intents to understand the behaviour of the signal and relevant background contributions by studying various event selections, aiming for an optimisation of the signal selection efficiency and purity. In addition, a cross section measurement is performed using the optimal selection. Background predictions and efficiency estimates are made based on simulation, properly scaled to data luminosity and corrected for differences in reconstruction efficiencies.

The structure of this document is as follows. Section 2 provides information about the data and simulated samples used for the analysis. Section 3 describes the event selection. The background estimation is documented in Section 4. Details of the process definition are given in Section 5, followed by a description of the cross section definition and the efficiency analysis. The results of the analysis are presented in Section 6. Section 7 is the summary of the analysis.

2 Data and Simulated Samples

The signal process in this analysis is the production of $t\bar{t}$ quark pairs followed by the top quark decays $t \to W^+ b$ and $\bar{t} \to W^- \bar{b}$, and subsequent leptonic $W^\pm$ boson decays, and a top quark radiating a Z^0 which decays to a lepton pair. Decays with intermediate taus and subsequent leptonic decay are also counted as signal. The event topology in leading order is thus 4 leptons, 2 bjets and missing E_T arising from the neutrinos (although the missing E_T is not considered in the analysis).

The data sample used during this analysis was recorded by the CMS experiment during the 2012 run at $\sqrt{s} = 8\,\text{TeV}$ and corresponds to an integrated luminosity of $\int \mathcal{L}dt = 19.789 \pm 0.871\,\text{fb}^{-1}$. These were collected with dilepton triggers (ee, eμ, $\mu\mu$) with no double counting ensured. The data samples were re-reconstructed on January 27, 2013, with improved calibrations and alignment.

The simulation samples used in the analysis are listed in Table 1. All cross sections are taken from [4], with the exception of $t\bar{t}H$, which is taken from [5], and $t\bar{t}$ and any unlisted samples which are from [6]. The $t\bar{t}H$ sample is for a Higgs mass of 125 GeV with the cross section calculated at NLO. The $t\bar{t}$ sample is valid for a top mass of 173.3 GeV, with the cross section calculated at NNLO. The main signal used is $t\bar{t}Z^0$. The main background considered is $Z^0Z^0 \to 4\ell$ with a requirement of $M_{Z^0} > 12\,\text{GeV}$. Other background contributions arise from WWZ, ZZZ and $t\bar{t}W^+W^-$. The $t\bar{t}H$ sample is also analysed as the process could be sensitive to this. To model the samples correctly they are reweighted for Pileup and a correction to the branching ratios of W decay in MADGRAPH. The detector effects are accounted for through η and p_T dependent scale factors for the leptons, and btagging corrections through random-number based tagging/untagging of b-, c- and light jets. The btag efficiencies are calculated using the $t\bar{t}Z^0$ simulation sample. The top dilepton analysis [7] shows that trigger efficiencies are high and scale factors for MC almost negligle. In 4 lepton events they are most probably negligible.

Table 1: Summary of all simulated data samples used in this analysis given with their cross sections at $\sqrt{s} = 8\,\text{TeV}$ and the number of events before event selection requirements are imposed. The uncertainties are taken to be 50%.

Sample	cross section [pb]	number of events
$t\bar{t}Z^0$ +jets	0.206	210160
$Z^0\,Z^0 \to 4\ell$	0.1769	4807893
$WZ \to 3l + \nu$ + jets	1.0575	2017979
WWZ + jets	0.0633	222234
ZZZ + jets	0.0192	224904
WWW + jets	0.08217	220549
$t\bar{t}$ + jets	245.8	6923750
$t\bar{t}\,W^\pm$ + jets	0.232	130108
$t\bar{t}W^+W^-$ + jets	0.002	217820
$t\bar{t}\,\gamma$+ jets	2.166	71598
$t\bar{t}H$	0.1293	995697

3 Event Selection and Optimisation

3.1 Event Selection

The event selection as found after several optimisations is documented in the following, including some descriptions of the optimisation studies. Signal events are required to have four spatially isolated leptons (electrons and muons) in the final state with $p_T > 20\,\text{GeV}$ and $\eta < |2.4|$

passing the trigger requirements of $p_T > 17\,\text{GeV}$ for the first lepton, and $p_T > 8\,\text{GeV}$ for the second lepton. This analysis uses the same reconstructed objects as the top dilepton differential cross section analysis [8][9]. The leptons originating from the Z^0 are identified by building all opposite sign same flavour (OSSF) pairs and taking the closest to the nominal Z^0 mass (91 GeV), requiring $M_{ll} > 12\,\text{GeV}$ since both simulated Z's in the $Z^0\,Z^0 \rightarrow 4\ell$ sample have $M_{Z^0} > 12\,\text{GeV}$ and to suppress low mass processes. The leptons associated with the top quarks are chosen from the remaining leptons, which are ordered in p_T, where an opposite sign (OS) pair decreasing in p_T with $M_{ll} > 12\,\text{GeV}$ is chosen. These selection requirements provide a good agreement between the data and simulation samples, as illustrated in Figures 2 and 3.

The jets are required to have $p_T > 30\,\text{GeV}$ and $\eta < |2.4|$. Using the combined secondary vertex (CSV) algorithm, the btag working point is chosen as the medium value of 0.679, providing a fake rate of about 1% for light jets, 15 - 20% for cjets, and an efficiency of 60 - 75% for bjets.

The event yields after selection are shown in Table 2, comparing the number of events in the data to the number of expected events in the simulation samples after each event selection step. The $t\bar{t}H$ sample is listed separately, and not considered in any calculations; it is also not shown in any figures. The event selection steps are as follows:

- 3 leptons: Events with at least 3 leptons passing the p_T, η and trigger requirements as above, with an OSSF pair forming the Z^0 under the constraints above.
- 4 leptons: Events with at least 4 leptons passing the p_T, η and trigger requirements, with an OSSF pair forming the Z^0 under the constraints above and the remaining two leptons fitting the top quark requirements as above.
- 1 jet: Events with 4 leptons as above with at least one jet fulfilling the jet p_T and η requirements.
- 1 jet + 1 btag: 4 lepton events with at least one jet as above, with one bjet with btag discriminator above the btag working point value.
- 2 jets: 4 lepton events with at least two jets fulfilling the jet p_T and η requirements.
- 2 jets + 1 btag: 4 lepton events with at least two jets as above, with one bjet with btag discriminator above the btag working point value.
- 2 jets + 2 btags: 4 lepton events with at least two jets and two btags as above.

Table 2 shows very good agreement between the data and simulated samples. There is a discrepancy at the 3 lepton stage, due the occurrence of more backgrounds not documented. Other simulation samples analysed for additional background contributions are found to be negligible after the 4 lepton event selection step. The Drell-Yan and multijet event samples show no 4 lepton final states events. Single top and antitop samples also provide no additional contribution. Finally no 4 lepton final states are observed in the $W \rightarrow \ell\nu$ and WW to all samples. Thus these samples are taken as negligible and not listed.

Once 4 leptons are required all processes not containing 4 real leptons are excluded, with the exception of a small contribution from $WZ \rightarrow 3l + \nu$, although this is suppressed by the requirement of 1 b-jet. This process provides insight into the fake rate in simulations in this analysis as any 4 lepton events from $WZ \rightarrow 3l + \nu$ will contain one fake lepton. From this it can be suggested that the lepton fake rate (due to non-isolated or misreconstructed leptons) is in general small due to the high p_T cut on the leptons and the requirements for lepton pairs, and is here neglected. At the 4 lepton stage the $Z^0\,Z^0 \rightarrow 4\ell$ process is dominant, but can be suppressed by the requirement of 1 b-jet, and heavy suppression can be obtained by requiring 2 b-jets. Once 2 b-jets are required, only 2 events survive but this stage is almost background-free. The good

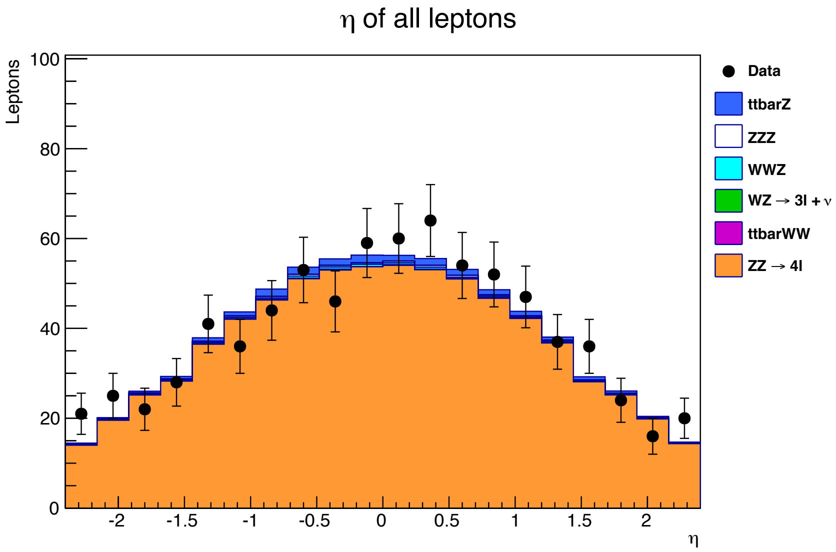

Figure 2: η of all leptons after the 4 lepton selection step. A good agreement is seen between simulation and data, supporting the event selection requirements.

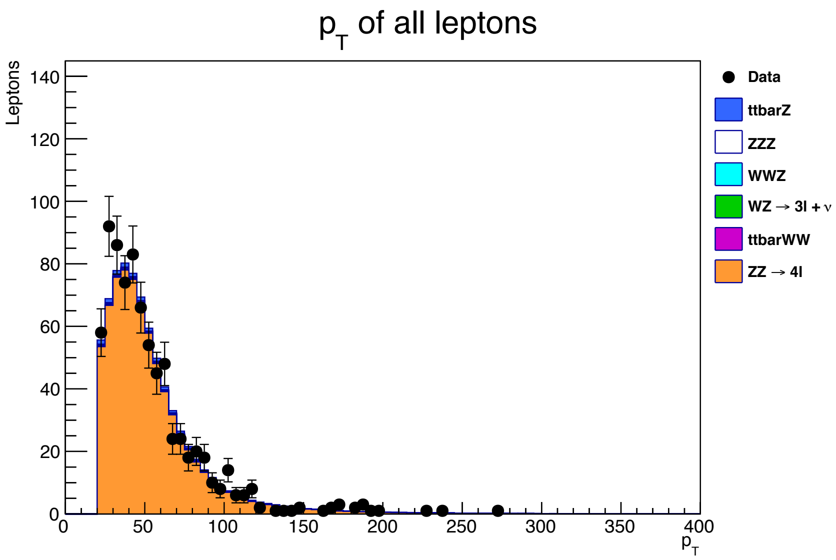

Figure 3: p_{T} of all leptons at the 4 leptons selection step. This shows agreement between simulation and data samples, supporting the event selection requirements.

Table 2: This table describes the event yield seen after each selection step in the analysis, where the event yields are weighted using the ratio of the luminosity of the data to the luminosity of the sample, and showing the statistical errors only. The $t\bar{t}H$ sample is not contained in the sum of backgrounds (Sum BG).

Sample	3 leptons	4 leptons	1 jet	+ 1 btag	2 jets	+ 1 btag	+ 2 btags
ZZ(4ℓ)	560 ± 0.7	185 ± 0.4	48.9 ± 0.2	2.54 ± 0.05	11.98 ± 0.10	1.10 ± 0.03	0.10 ± 0.01
WZ($3\ell\nu$)	2078 ± 4.9	0.40 ± 0.07	0.18 ± 0.05	0.00	0.09 ± 0.03	0.00	0.00
WWZ	15 ± 0.3	1.40 ± 0.10	0.72 ± 0.07	0.13 ± 0.03	0.32 ± 0.05	0.08 ± 0.02	0.01 ± 0.008
ZZZ	3.7 ± 0.09	1.38 ± 0.05	0.98 ± 0.04	0.16 ± 0.02	0.50 ± 0.03	0.10 ± 0.01	0.02 ± 0.006
WWW	5.1 ± 0.2	0.00	0.00	0.00	0.00	0.00	0.00
$t\bar{t}$	126 ± 9.6	0.00	0.00	0.00	0.00	0.00	0.00
$t\bar{t}\,W^{\pm}$	15 ± 0.8	0.00	0.00	0.00	0.00	0.00	0.00
$t\bar{t}W^+W^-$	0.3 ± 0.01	0.03 ± 0.002	0.03 ± 0.002	0.02 ± 0.002	0.02 ± 0.002	0.02 ± 0.002	0.01 ± 0.001
$t\bar{t}\,\gamma$	4.4 ± 1.7	0.00	0.00	0.00	0.00	0.00	0.00
$t\bar{t}Z^0$ signal	50 ± 1.0	4.44 ± 0.30	4.35 ± 0.3	3.21 ± 0.26	3.28 ± 0.26	2.63 ± 0.24	1.19 ± 0.16
Sum BG	2808.32	189.04	50.77	2.85	12.91	1.30	0.14
+ signal	2858.35	193.48	55.12	6.06	16.19	3.92	1.33
Data	5856 ± 76	196 ± 14	42 ± 6.48	7 ± 2.65	13 ± 3.61	6 ± 2.45	2 ± 1.41
$t\bar{t}H$	6.78 ± 0.14	0.43 ± 0.03	0.41 ± 0.03	0.32 ± 0.03	0.34 ± 0.03	0.28 ± 0.03	0.10 ± 0.02

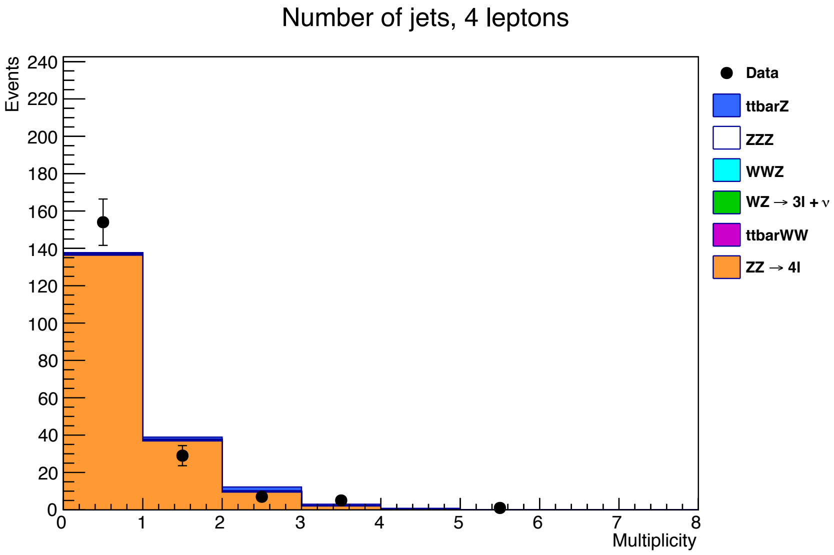

Figure 4: Jet multiplicity at the 4 lepton event selection stage.

agreement between data and simulation in the jet and bjet multiplicity after the 4 lepton and the 4 lepton + 1 jet event selection steps can be seen in Figures 4, 5, 6 and 7. Additional control distributions at different selection steps can be found in Appendix A. About the $t\bar{t}H$, it can be observed from Table 2 that it is a non-negligible contribution in all steps with jets.

3.2 Selection Optimisation

An investigation is made into the p_T dependence of the analysis by lowering the p_T lower limit on the leptons. This only affects the 3rd and 4th leptons, as the two leading leptons never have p_T below 20 GeV (see Figures 18 and 19 in Appendix A). By lowering the p_T lower limit to $p_T > 10$ there are additional contributions from the 3rd and 4th leptons, and at $p_T > 5$ additional contributions arise only from the 4th lepton. This p_T lowering introduces more

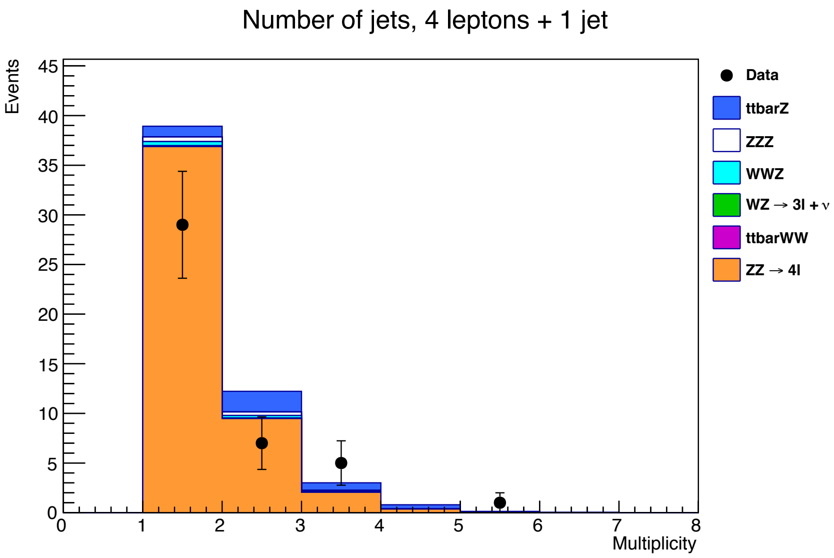

Figure 5: Jet multiplicity at the 4 leptons + 1 jet event selection stage.

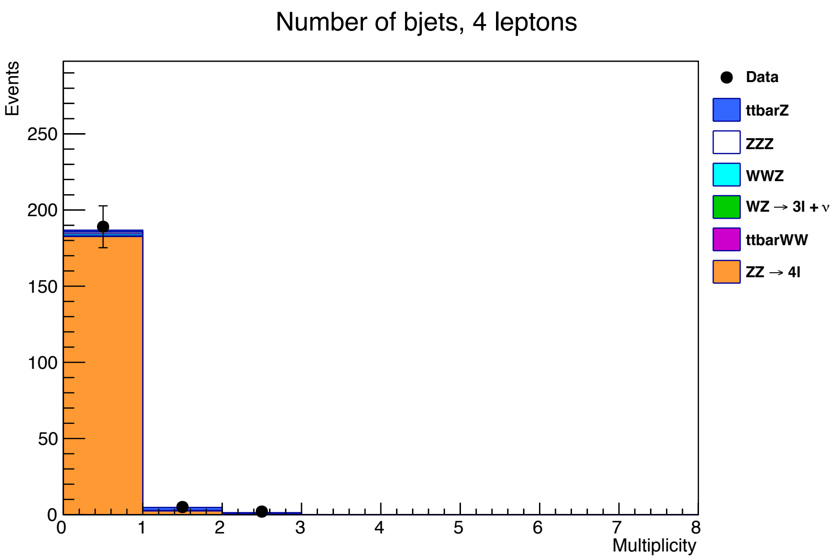

Figure 6: The b-jet multiplicity at the 4 lepton event selection stage.

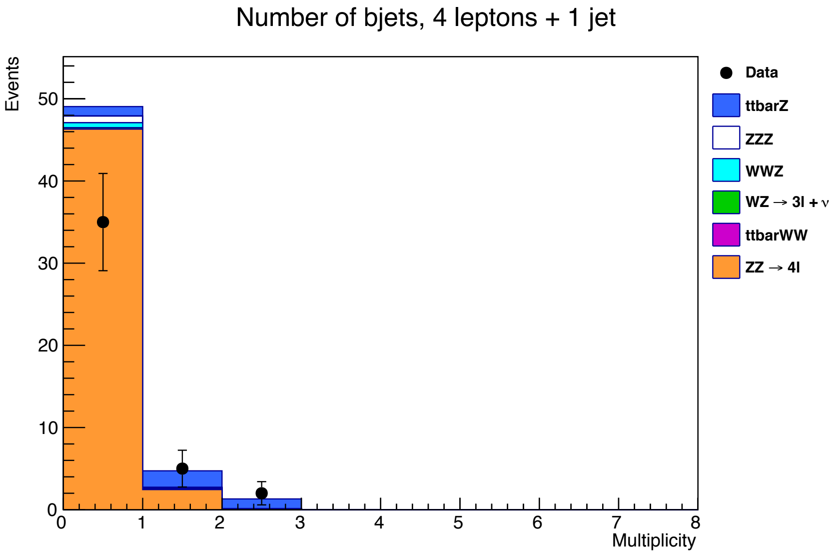

Figure 7: The b-jet multiplicty at the 4 leptons + 1 jet event selection stage.

statistics but simultaneously more fakes and is therefore unreliable.

The medium btag working point of 0.679 is used in this analysis. This is supported by studies of optimisation of the btag working point by comparing the btag discriminator plots of the background sample and the signal sample. Additionally a study of efficiency with respect to purity is conducted on the signal sample which further confirms the decision of the medium btag working point. The loose working point shows clearly worse performance in suppressing backgrounds not containing a $t\bar{t}$ system.

To choose the optimal step for a cross section calculated of this process a signal selection efficiency against purity study is plotted, as seen in Figure 8, for the final definition of the selection steps. The step with 2 jets + 1 btag shows the highest efficiency times purity. However it is informative to investigate the step 1 jet + 1 btag, which performs slightly worse, but has the higher efficiency. The dominant ZZ background shows up mainly in events where the OS lepton pair is also of same flavour (see Figure 9). Furthermore, since we aim to investigate $t\bar{t}Z^0$, the sensitivity to $t\bar{t}H$ should be reduced, and this cannot be done by jet or bjet requirements. The selection of a dilepton mass window for the Z^0 boson then needs to be made to suppress the $t\bar{t}H$, and this is done for the OSSF pair for a wide window of 60 - 120 GeV and a narrow window of $76 - 106$ GeV, and the latter is chosen for the final selection requirements. Additionally, for further suppression of ZZ, a veto is applied in case the OS lepton pair associated with the top system is also of same flavour and within the Z mass window. These steps are exposed in the next section.

4 Background Estimation

The main background contribution arises from the ZZ to 4 lepton process, with small contributions from the WWZ, ZZZ and $t\bar{t}\,W^+\,W^-$ processes. Figures 10 and 11 support the selection of 4 leptons, 1 jet + 1 btag as Figure 10 shows a sharp peak at the Z mass with a strong signal contribution, and Figure 11 shows a shallow peak around the Z mass dominantly from the ZZ to 4ℓ process; both figures show decent data-to-simulation agreement.

To further suppress backgrounds two additional event selection steps are imposed:

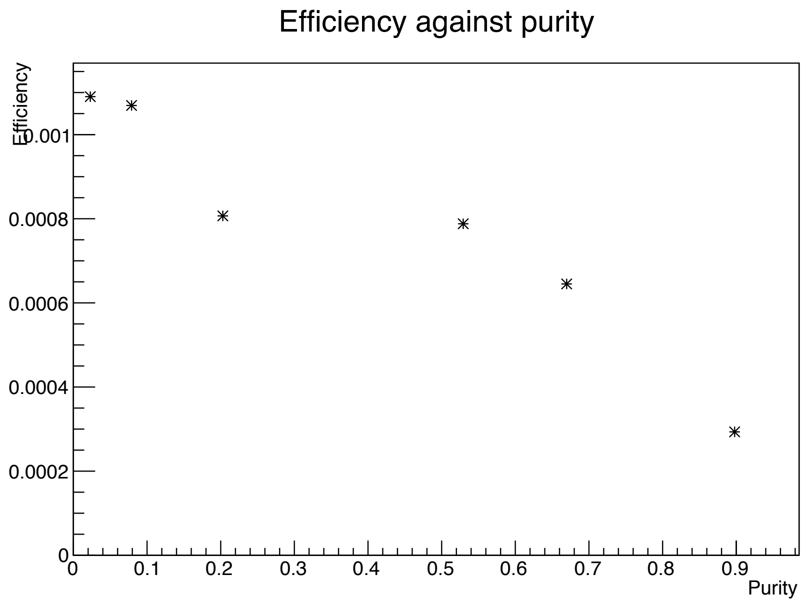

Figure 8: Dependence of efficiency on purity, where efficiency is calculated using Equation 3, and purity is defined as the signal events divided by the sum of the signal and background. From left to right the markers represent the event selection stages: 4 leptons, 4 leptons + 1 jet, 4 leptons + 2 jets, 4 leptons + 1 jet + 1 btag, 4 leptons + 2 jets + 1 btag, 4 leptons + 2 jets + 2 btags. Although the 4 leptons + 2 jets + 1 btag stage may appear the optimum selection stage, the statistics are not high enough here, and additionally the $t\bar{t}H$ background is not well enough suppressed. From this, it is decided to use 4 leptons + 1 jet + 1 btag and modify the lepton requirementss rather than the jet requirements to suppress $t\bar{t}H$ and other backgrounds.

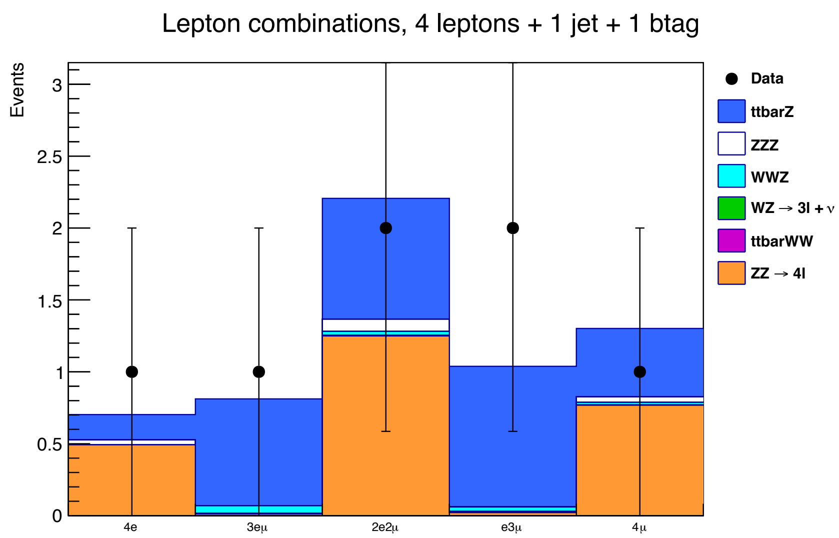

Figure 9: Number of events in the 5 lepton categories at the 4 lepton + 1 jet + 1 btag selection stage. It can be seen that the ZZ background occurs in same flavour combinations as expected, whereas there is very little background in the 3eμ and e3μ categories.

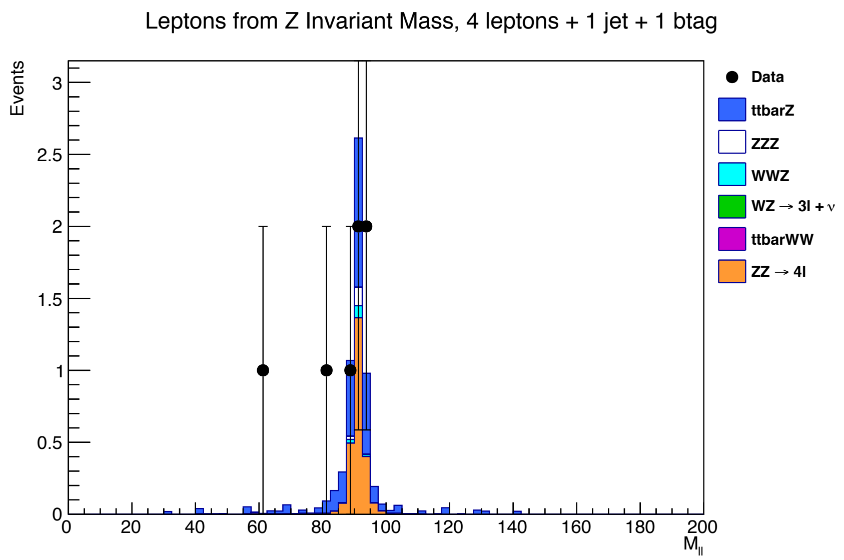

Figure 10: The dilepton invariant mass composed of the two leptons identified as originating from the Z^0 boson. This shows a sharp peak around the Z^0 mass with very little background.

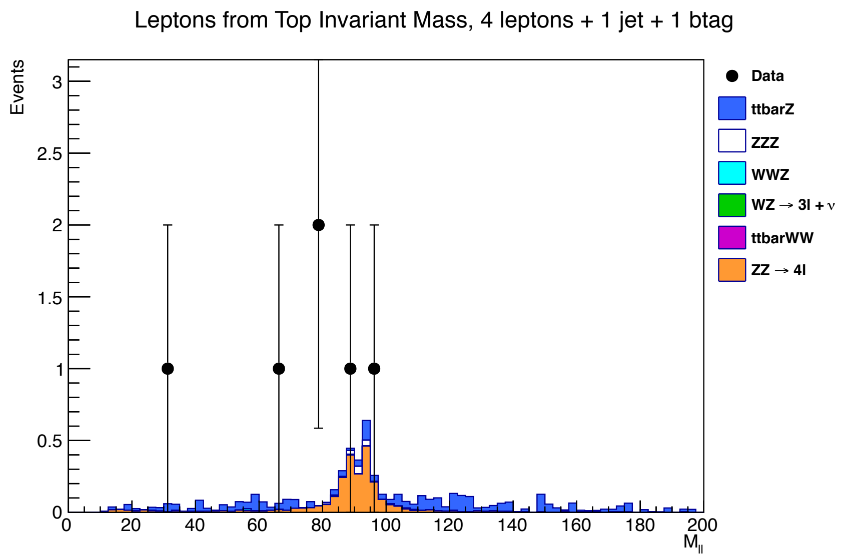

Figure 11: The dilepton invariant mass composed of the two leptons associated with the top quarks.

- Z window: Events with 4 leptons, 1 jet + 1 btag, where the OSSF lepton pair is in the Z mass window of $76 < M_{\ell\ell} < 106$.
- 2nd Z veto: As above, but in addition the OS lepton pair required to be outside the Z mass window ($M_{\ell\ell} < 76$ or $M_{\ell\ell} > 106$) if they are the same flavour.

The Z window cut is important for the rejection of $t\bar{t}H$ events, and also removes a considerable amount $t\bar{t}W^+W^-$ events. The 2nd Z veto stage rejects ZZ events and reduces the contribution from ZZZ processes. The event yield from these selection steps can be seen in Table 3. The 2nd Z veto is the last event selection stage and from now will be referred to as the final selection. We observe $N_{\rm obs} = 3$ events in the data; Figure 12 shows the lepton flavour composition.

The final background estimate is taken from simulation for the final selection. An uncertainty of 50% is assigned to all background processes to cover cross section uncertainties, as in the $t\bar{t}Z^0$ measurement at 7 TeV [2]. Statistical (5%) and luminosity (4.4%) uncertainties are much smaller and not considered. The background is taken without $t\bar{t}H$ and yields $N_{\rm bkg} = 0.61 \pm 0.31$. The $t\bar{t}H$ process is not measured so far, but the latest upper limit is 3.4 times the SM prediction [10]. Including the SM prediction would lead to a background of $N_{\rm bkg} = 0.77^{+0.85}_{-0.47}$ events.

Table 3: This table provides a final background estimate using the simulated samples, showing statistical uncertainties only. $t\bar{t}H$ is not included in the background sum (Sum BG).

Sample	1 jet + 1 btag, Z mass window	+ 2nd Z^0 veto (final selection)
ZZ(4ℓ)	2.49 ± 0.05	0.48 ± 0.02
WWZ	0.12 ± 0.03	0.12 ± 0.02
ZZZ	0.16 ± 0.02	0.008 ± 0.004
$t\bar{t}W^+W^-$	0.007 ± 0.001	0.007 ± 0.001
$t\bar{t}Z^0$ signal	2.84 ± 0.24	2.57 ± 0.23
Sum BG	2.78	0.61
+ signal	5.62	3.18
Data	6 ± 2.45	3 ± 1.73
$t\bar{t}H$	0.17 ± 0.02	0.16 ± 0.02

5 Process Definition

5.1 Cross Section

A measurement is made of the production cross section of $t\bar{t}Z^0$ events in pp collisions at $\sqrt{s} =$ 8 TeV, i.e.

$$\sigma^{t\bar{t}Z^0} = \sigma\left(pp \to t\bar{t}Z^0 + X\right) . \tag{1}$$

The calculation of the cross section is performed using Equation 2; $N_{\rm obs}$, $N_{\rm sig}$ and $N_{\rm bkg}$ are defined as the number of events in the data, the signal, and the background respectively and $N_{\rm sig} = N_{\rm obs} - N_{\rm bkg}$. $\epsilon_{\rm tot}$ is defined as the total event selection efficiency, the calculation for which can be found in Equation 3, and $\int \mathcal{L}{\rm d}t$ as the integrated luminosity of the data sample used.

$$\sigma = \frac{N_{\rm sig}}{\epsilon_{\rm tot} \cdot \int \mathcal{L}{\rm d}t} = \frac{N_{\rm obs} - N_{\rm bkg}}{\epsilon_{\rm tot} \cdot \int \mathcal{L}{\rm d}t} . \tag{2}$$

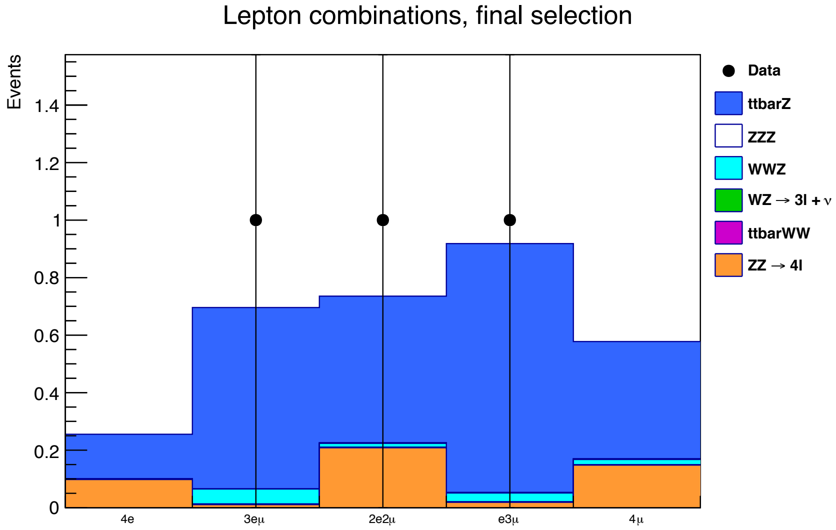

Figure 12: Number of events in the 5 lepton categories at the final selection stage with 4 leptons + 1 jet + 1 btag + Z window + 2nd Z veto. Here the backgrounds are greatly reduced and there are three data events, 1 in the 3eμ category, 1 in the 2e2μ, and one in the e3μ. The $t\bar{t}Z^0$ process is clearly dominant here.

5.2 Efficiency

The efficiency can be calculated for the $t\bar{t}Z^0$ sample corrected for lepton reconstruction and btag efficiencies as Equation 3 shows.

$$\epsilon_{\text{tot}} = \frac{\text{Number of events at final selection}}{\text{Number of all events}} \tag{3}$$

The efficiency at the final selection step is calculated using Equation 3 as

$$\epsilon_{\text{tot}} = 0.00063106 \pm 0.00005478 \, (\text{stat.}) \,, \tag{4}$$

where the branching ratios for $t\bar{t}Z^0 \rightarrow 2\ell 2bZ^0$ ($\approx$5%) and $Z^0 \rightarrow \ell\ell$ ($\approx$6%) are included.

B-tagging efficiencies in MC are estimated at the modified step of full dilepton selection + 1 jet, to be close to the final kinematics whilst keeping high statistics. Potentially calculating these b-tagging efficiencies at a 3 leptons + 1 jet step could provide an optimisation, but this is not studied.

5.3 Systematic effects

Table 4 shows the variation of the cross section and the uncertainty assigned due to systematic effects. To produce these, the analysis is re-run with varied effects within uncertainties up and down. The cross section is recalculated and the difference taken with the nominal cross section. The assigned uncertainty is chosen as the up or down variation with the largest amplitude, rounded to the full percentage. This is a conservative estimate and should cover neglected uncertainties, such as the fake rate, charge misassignments and trigger efficiency uncertainties. Note that these are not the latest scale factors for the leptons and jet energy corrections. Acceptance effects from the extrapolation of the measured phase space to the one of the cross section definition are not studied and not considered.

Table 4: Uncertainties on the cross section measurement from different systematic sources. The combined value, which is used in calculations, is the sum in quadrature of the assigned uncertainties. The variation up and down are the sum in quadrature of all the positive and negative values respectively.

Systematic	Up (%)	Down (%)	Assigned uncertainty (%)
Pile up	$+0.492$	-0.083	1
Lepton efficiencies	-7.819	$+8.474$	9
Jet energy resolution	$+0.205$	-0.115	1
Jet energy scale	-0.525	$+0.641$	1
Btagging efficiencies	-4.224	$+3.302$	5
Mistagging efficiencies	-0.696	$+1.085$	1
All combined			11
Variation up			+9.20
Variation down			-8.93

6 Results and discussion

The measurement of the cross section of $t\bar{t}Z^0$ production defined in Equation 1 at the final selection step calculated using Equation 2 is

$$\sigma^{t\bar{t}Z^0} = 191.187 \pm 138.793 \text{ (stat.)} \pm 37.335 \text{ (syst.) fb}\,. \tag{5}$$

The precision is dominated by the statistical uncertainty. It shows excellent agreement with the theory value calculated at NLO [3] of $\sigma^{t\bar{t}Z^0}_{\text{theo}} = 206^{+19}_{-24}$ fb.

After requiring 4 leptons, 2 jets and 2 btags, 2 events remain within the data sample (see Table 2). Of these, one event fits to the additional requirements for the dilepton masses. This selection has very low background contribution and a strong signal expected. This $t\bar{t}Z^0$ event candidate has a Z mass of 93.27, a dilepton mass of the top system of 30.94 and jet multiplicity of 3. The two leptons originating from the Z are identified as muons, and the leptons associated with the top quarks are a muon and a positron. This event as reconstructed in Event Viewer is displayed in Figures 13, 14 and 15. All properties are listed in Table 5. Of course there is a small remaining possibility that it is one of the rare backgrounds, e.g. a ZZ event with one $Z^0 \to \tau\tau \to e\mu +$ neutrinos, an event containing fake leptons, or even a real Higgs event. However, this event survives the strict requirements of 4 leptons, 2 jets, 2 btags, the Z window and 2nd Z veto, where the expectation for background is 0.0003 and $t\bar{t}Z^0$ is 0.33. The only other significant contribution could be $t\bar{t}H$ with an expected yield of 0.014.

Table 5: This table presents the details of the $t\bar{t}Z^0$ event candidate.

Event number: 123865322	Lumiblock: 78	Run number: 191810	Missing ET: 114.308	Jet multiplicity: 3
Object	Mass (GeV)	p_T (GeV)	η	btag
Z^0	93.274	113.414	-1.05095	n/a
Top dilepton system	30.9396	n/a	n/a	n/a
Z^0 Lepton 1	n/a	120.191	-0.955953	n/a
Z^0 Lepton 2	n/a	23.3815	-0.382538	n/a
$t\bar{t}$ Lepton 1	n/a	38.1706	-1.38417	n/a
$t\bar{t}$ Lepton 2	n/a	29.8623	-0.903026	n/a
Jet 1	n/a	162.477	-1.24913	0.883643
Jet 2	n/a	124.14	-0.318806	0.830203
Jet 3	n/a	58.9966	2.24644	0.119958

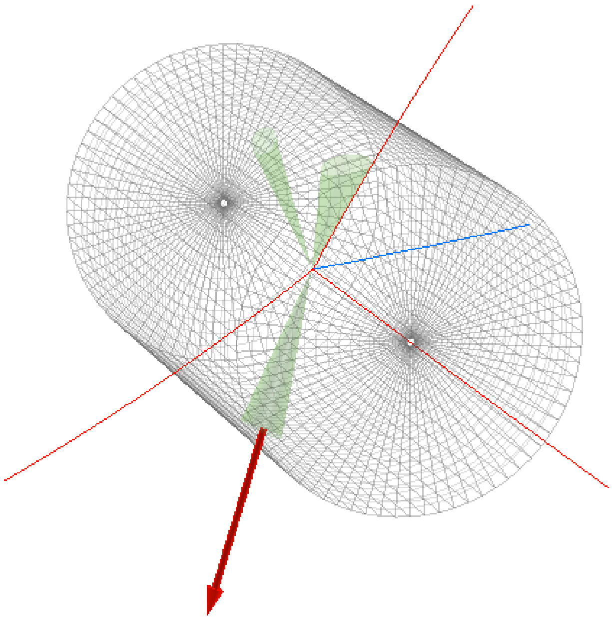

Figure 13: The event that fits the $t\bar{t}Z^0$ requirements. The red lines represent muons, the blue line an electron, the green cones jets, and the red arrow the missing transverse energy (the neutrinos).

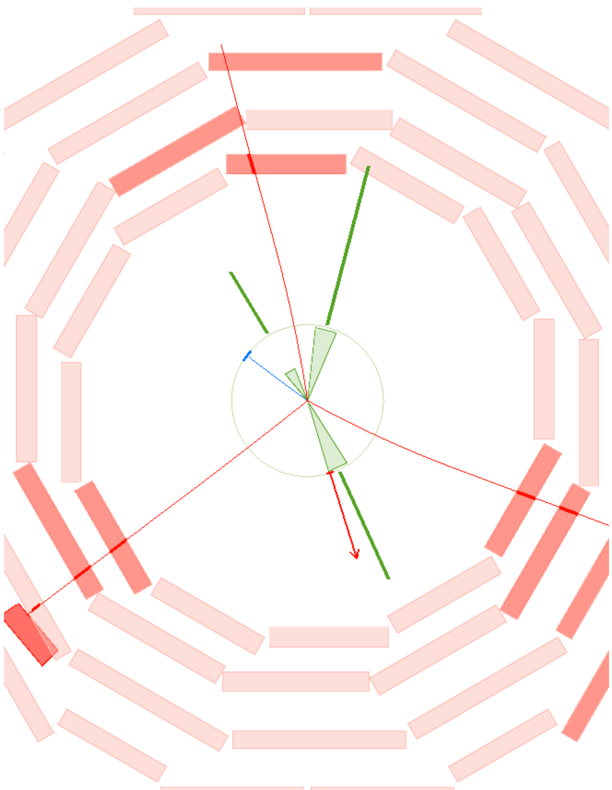

Figure 14: The event along the $\rho - \phi$ view.

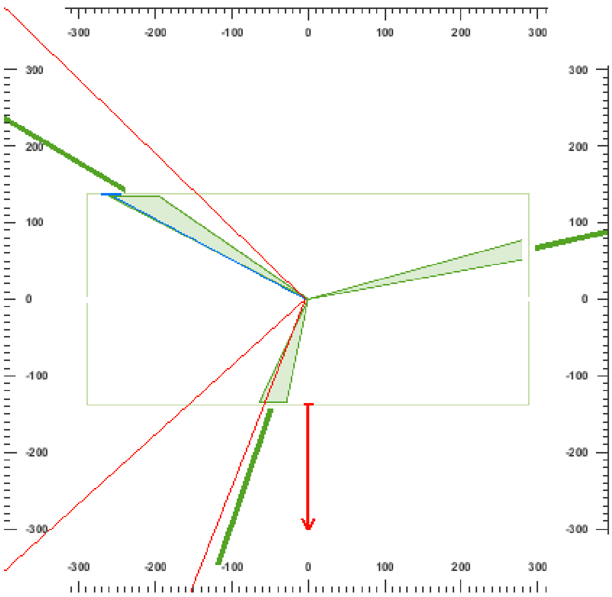

Figure 15: The event along the $\rho - \mathrm{Z}$ view.

6.1 Combined cross section measurement from lepton flavour categories

The cross section is also calculated by combining the cross sections from the individual lepton flavour categories seen in Figure 12. This is done using a combine tool which determines a combined fit with likelihood maximisation. The cross section can be determined using this method as

$$\sigma_{\mathrm{comb}}^{\mathrm{t\bar{t}Z^0}} = 204.6 \pm 136.4\,(\mathrm{stat.}) \pm 23.5\,(\mathrm{syst.})\,\mathrm{fb}\,. \tag{6}$$

The systematic error only has a small contribution; excluding it only effects the relative error by 1%. The statistical error is reduced by 10% using this method. If the $\mathrm{t\bar{t}H}$ sample is included the cross section decreases to

$$\sigma_{\mathrm{inc\ t\bar{t}H}}^{\mathrm{t\bar{t}Z^0}} = 192.2 \pm 137.0\,(\mathrm{stat.}) \pm 25.0\,(\mathrm{syst.})\,\mathrm{fb}\,. \tag{7}$$

6.2 Potential optimisations and extensions of the analysis

It would be interesting to define the visible cross section reflecting the measured phase space for the calculations, and this could potentially improve the analysis. Additionally the analysis could be conducted using a kinematic reconstruction of the $\mathrm{t\bar{t}}$ system [8][9], and measuring an unbiased peak in the Z mass spectrum instead of identifying the Z directly. The missing E_{T} could be investigated to refine the analysis. A treatment of the neglected uncertainties, e.g. acceptance uncertainties or corrections, could be conducted, and a precise treatment of non-neglected uncertainties. Furthermore, the statistical error could be calculated with Poissonian statistics, assuming the SM prediction is correct. Observing the $\mu\mu$ee, $\mu\mu\mu$e and eeeμ combinations could be interesting due to the high level of signal (see Figure 12), and further these could be disentangled using $M_{\ell\mathrm{b}}$.

At $\sqrt{s} = 13\,\mathrm{TeV}$, with higher statistics, it may be interesting to make a combined $\mathrm{t\bar{t}H}$, $\mathrm{t\bar{t}Z^0}$ measurement, or to measure $\mathrm{t\bar{t}H}$ multilepton final states in a cut-based analysis, e.g. by requiring both dileptons to be outside the Z mass window.

7 Summary

A study is made of 4 lepton final states in $t\bar{t}Z^0$ production at $\sqrt{s} = 8$ TeV and $\int \mathcal{L}dt = 19.8\,\text{fb}^{-1}$. This analysis focuses on gaining insight into the signal and background contributions, and various selections are studied in order to optimise the $t\bar{t}Z^0$ signal selection efficiencies and purities. The final selection is chosen as requiring 4 leptons, 1 jet and 1 btag, imposing a Z mass window and a veto on the 2nd Z. A measurement is made of the cross section of the $t\bar{t}Z^0$ process using event selection steps chosen by optimising the analysis, and is calculated as $\sigma_{\text{inc}}^{t\bar{t}Z^0} = 191 \pm 144$ fb. The measurement is strongly limited by the statistical precision, but this will change in the next LHC run period, when collisions will be provided at $\sqrt{s} = 13$ TeV. This measurement shows agreement with the theoretical prediction of $\sigma_{\text{inc}}^{t\bar{t}Z^0} = 206$ fb. Exactly one event is found in a very strict selection, where almost no background is predicted.

References

[1] CMS Collaboration, "The CMS experiment at the CERN LHC", *JINST* **3** (2008) S08004, doi:10.1088/1748-0221/3/08/S08004.

[2] CMS Collaboration, "Measurement of associated production of vector bosons and top quark-antiquark pairs at $\sqrt{s} = 7$ TeV", *Phys.Rev.Lett.* **110** (2013) 172002, doi:10.1103/PhysRevLett.110.172002, arXiv:1303.3239.

[3] M. Garzelli, A. Kardos, C. Papadopoulos, and Z. Trocsanyi, "$t\bar{t}W^{\pm}$ and $t\bar{t}Z^{0}$ Hadroproduction at NLO accuracy in QCD with Parton Shower and Hadronization effects", *JHEP* **1211** (2012) 056, doi:10.1007/JHEP11(2012)056, arXiv:1208.2665.

[4] Homepage, "CMS Top Quark Properties Subgroup Meeting on July 5th 2013",. https://indico.cern.ch/conferenceDisplay.py?confId=260044.

[5] Homepage, "SM Higgs production cross sections at $\sqrt{s} = 8$ TeV",. https://twiki.cern.ch/twiki/bin/view/LHCPhysics/CERNYellowReportPageAt8TeV.

[6] Homepage, "Standard Model Cross Sections for CMS at 8 TeV",. https://twiki.cern.ch/twiki/bin/viewauth/CMS/StandardModelCrossSectionsat8TeV.

[7] J. Kieseler and C. Diez Pardos, "Dilepton trigger and lepton identification efficiencies for the top quark pair production cross section measurement at 8 TeV in the dilepton decay channel",. Analysis Note 2012-389.

[8] CMS Collaboration, "Measurement of the differential $t\bar{t}$ cross section in the dilepton channel at 8 TeV", Technical Report CMS-PAS-TOP-12-028, CERN, Geneva, (2013).

[9] M. Aldaya et al., "Measurement of differential top-quark pair production cross sections in the dilepton final state at $\sqrt{s} = 8$ TeV",. Analysis Note 2012-388.

[10] CMS Collaboration, "Search for Higgs Boson Production in Association with a Top-Quark Pair and Decaying to Bottom Quarks or Tau Leptons", Technical Report CMS-PAS-HIG-13-019, CERN, Geneva, (2013).

A Additional Control Distributions

Additional control distributions at various event selection stages are presented here. The captions and titles provide event selection stages and any important information.

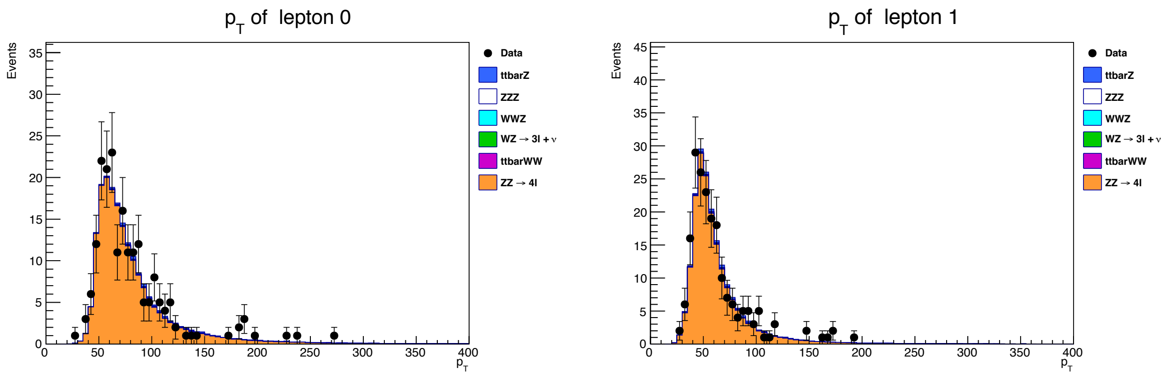

Figure 16: The p_T distribution of the leading lepton (left), and the next leading lepton (right) at the 4 lepton event selection step.

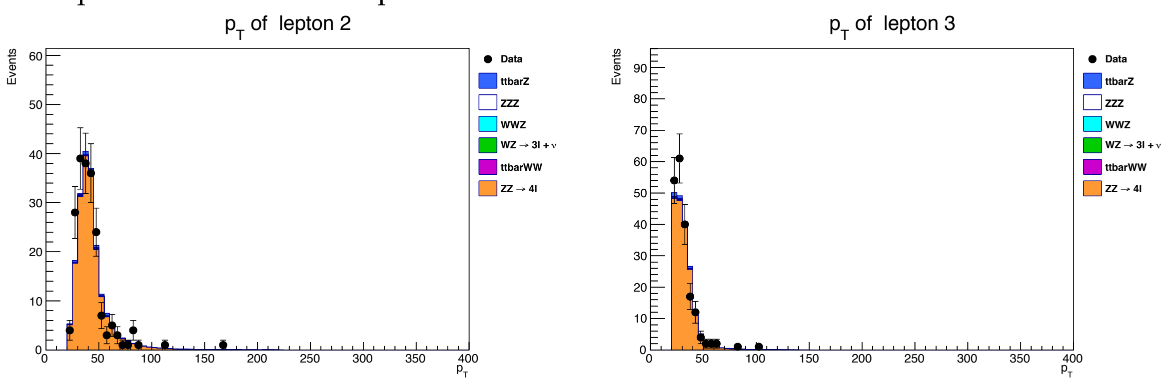

Figure 17: The p_T distribution of the third lepton (left), and the fourth lepton (right) at the 4 lepton event selection step.

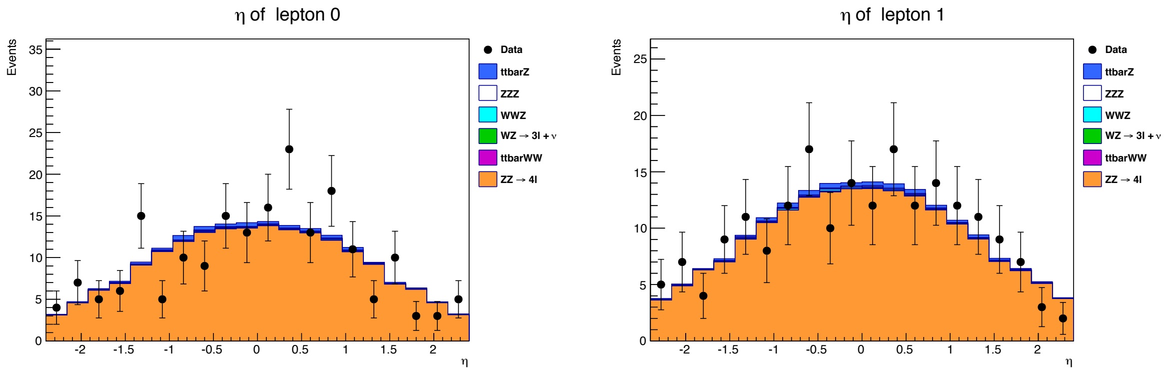

Figure 18: The η distribution of the leading lepton (left), and the next leading lepton (right) at the 4 lepton event selection step.

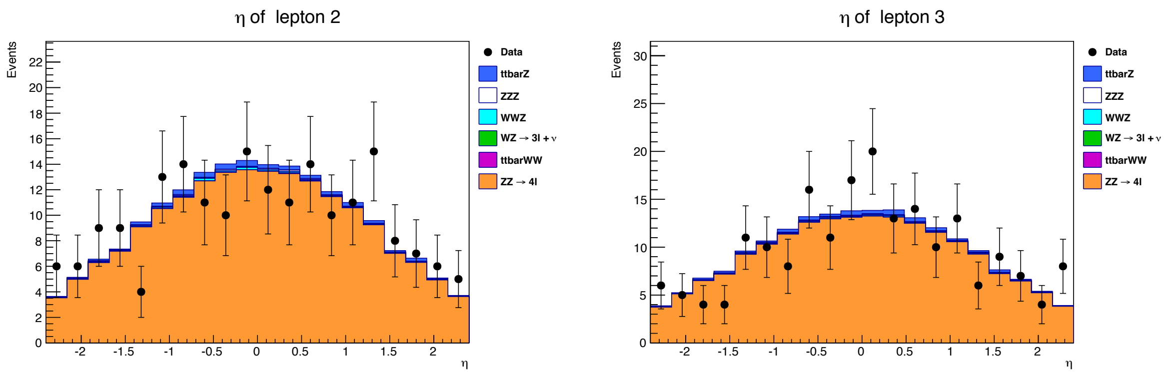

Figure 19: The η distribution of the third lepton (left), and the fourth lepton (right) at the 4 lepton event selection step.

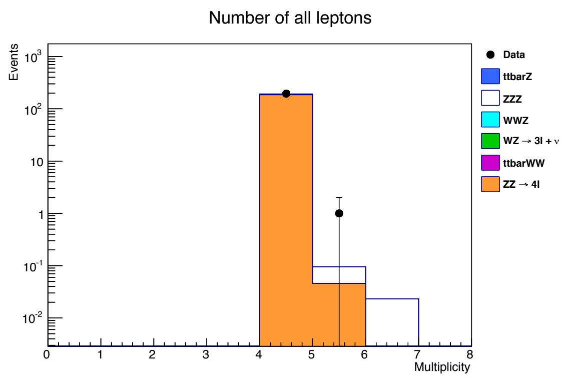

Figure 20: The lepton multiplicity on a log scale at the 4 lepton event selection step. It can be seen that the ZZZ sample provides some 5- and 6-lepton events. The data sample shows one 5-lepton event.

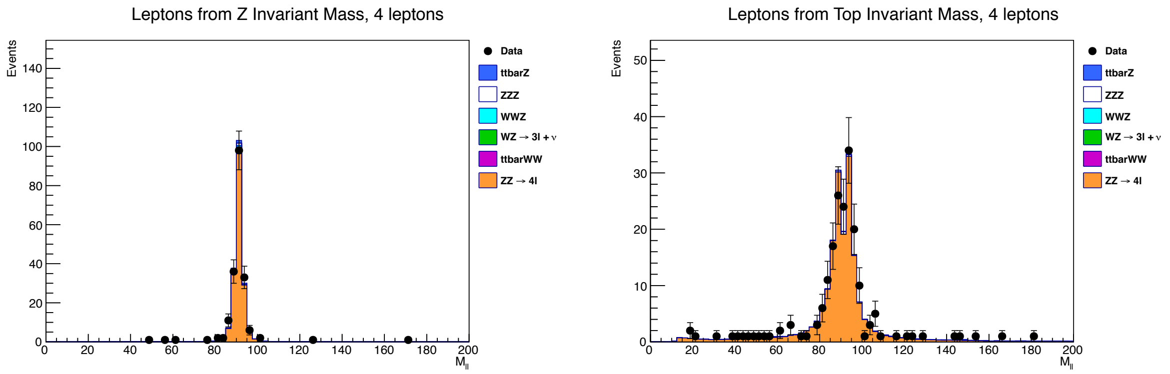

Figure 21: Invariant mass of the Z system (left) and the top system (right) after requiring 4 leptons.

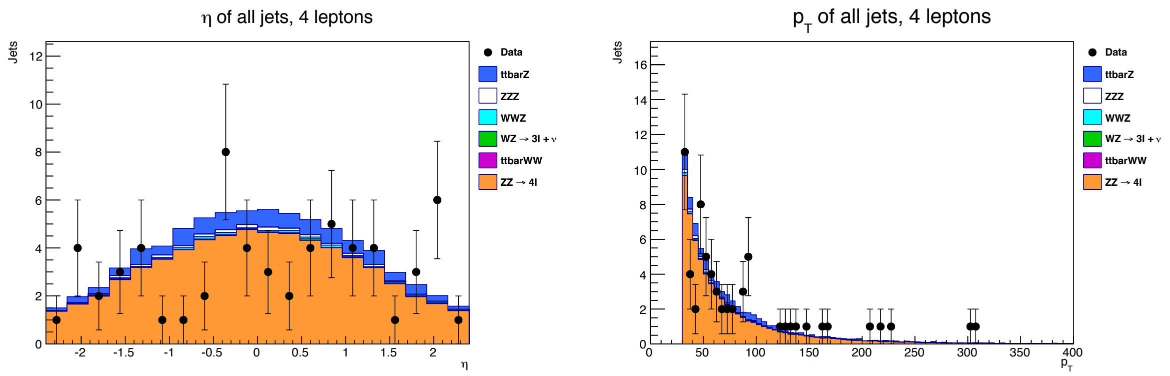

Figure 22: The distribution of η (left) and p_{T} (right) for all jets after requiring 4 leptons.

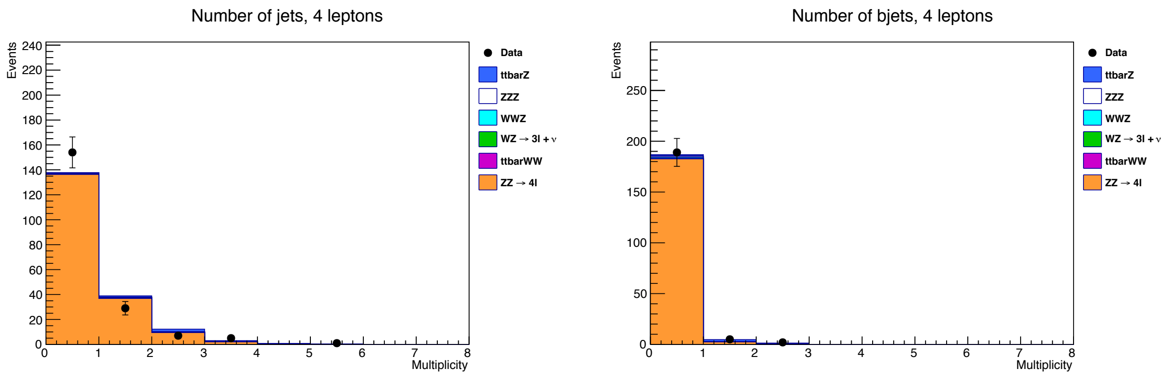

Figure 23: The jet and bjet multiplicity at the 4 lepton event selection step.

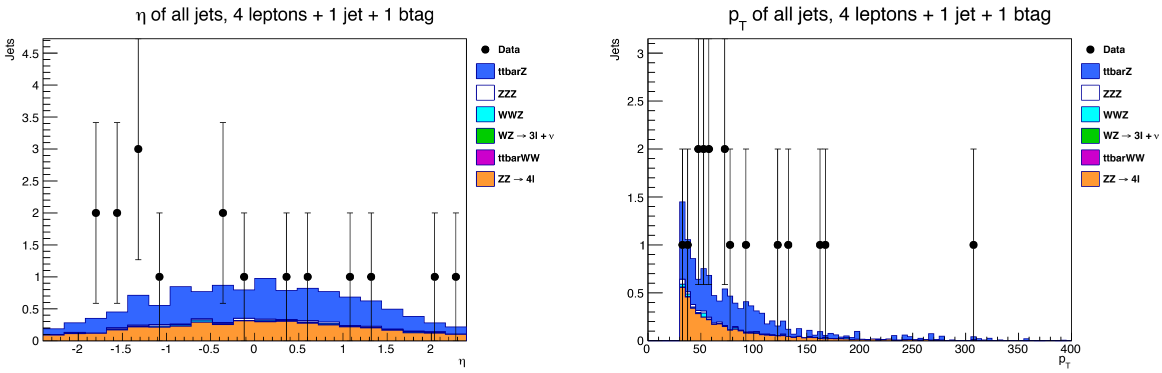

Figure 24: The distribution of η (left) and p_{T} (right) for all jets after requiring 4 leptons, 1 jet and 1 btag.

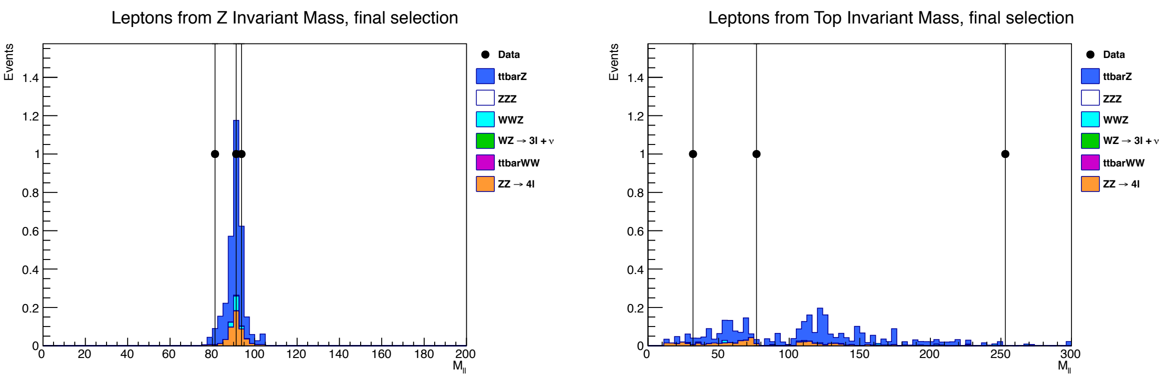

Figure 25: Invariant mass of the Z system (left) and the top system (right) after requiring 4 leptons, 1 jet, 1 btag, the Z window and the 2nd Z veto (final selection requirements).

B Alternative Versions of Tables

Table 6: Summary of all data samples used in this analysis given with the number of events before event selection requirements.

Sample	number of events
ee_run2012A	9522277
ee_run2012B	21474290
ee_run2012C	32537540
ee_run2012D	32569000
emu_run2012A	1939498
emu_run2012B	13525360
emu_run2012C	20086020
emu_run2012D	20902360
mumu_run2012A	4784511
mumu_run2012B	26084710
mumu_run2012C	35455700
mumu_run2012D	35891540

Table 7: Summary of all simulated data samples used in this analysis given with their cross sections at $\sqrt{s} = 8\,\text{TeV}$ and the number of events before event selection cuts are made. The name of each sample is appended with /Summer12_DR53x-PU_S10_STARTS53_V7A-v1.

Sample	cross section	number of events
TTZJets_8TeV-madgraph_v2	0.208	210160
ZZJetsTo4L_TuneZ2star_8TeV-madgraph-tauola	0.1769	4807893
WZJetsTo3LNu_TuneZ2_8TeV-madgraph	1.0575	2017979
WWZNoGstarJets_8TeV-madgraph	0.0633	222234
ZZZNoGstarJets_8TeV-madgraph	0.0192	224904
WWWJets_8TeV-madgraph	0.08217	220549
TTJets_MassiveBinDECAY_TuneZ2star_8TeV-madgraph-tauola	245.8 ± 0.00	6923750
TTWJets_8TeV-madgraph	0.232	130108
TTWWJets_8TeV-madgraph	0.002	217820
TTGJets_8TeV-madgraph	2.166	71598
TTH_Inclusive_M-125_8TeV_pythia6	0.1293 ± 0.00	995697

Table 8: This table describes the event yield seen after each selection step in the analysis, where the event yields are weighted using the ratio of the luminosity of the data to the luminosity of the sample, and showing the statistical errors only. The $t\bar{t}H$ sample is not contained in the sum of backgrounds (Sum BG).

Sample	4 leptons	1 jet	+ 1 btag	2 jets	+ 1 btag	+ 2 btags
$ZZ(4\ell)$	185 ± 0.4	48.9 ± 0.2	2.54 ± 0.05	11.98 ± 0.10	1.10 ± 0.03	0.10 ± 0.01
$WZ(3\ell\nu)$	0.40 ± 0.07	0.18 ± 0.05	0.00	0.09 ± 0.03	0.00	0.00
WWZ	1.40 ± 0.10	0.72 ± 0.07	0.13 ± 0.03	0.32 ± 0.05	0.08 ± 0.02	0.01 ± 0.008
ZZZ	1.38 ± 0.05	0.98 ± 0.04	0.16 ± 0.02	0.50 ± 0.03	0.10 ± 0.01	0.02 ± 0.006
$t\bar{t}W^+W^-$	0.03 ± 0.002	0.03 ± 0.002	0.02 ± 0.002	0.02 ± 0.002	0.02 ± 0.002	0.01 ± 0.001
$t\bar{t}Z^0$ signal	4.44 ± 0.30	4.35 ± 0.3	3.21 ± 0.26	3.28 ± 0.26	2.63 ± 0.24	1.19 ± 0.16
Sum BG	189.04	50.77	2.85	12.91	1.30	0.14
+ signal	193.48	55.12	6.06	16.19	3.92	1.33
Data	196 ± 14	42 ± 6.48	7 ± 2.65	13 ± 3.61	6 ± 2.45	2 ± 1.41
$t\bar{t}H$	0.43 ± 0.03	0.41 ± 0.03	0.32 ± 0.03	0.34 ± 0.03	0.28 ± 0.03	0.10 ± 0.02

Table 9: Uncertainties on the cross section measurement from different systematic sources. The combined value, which is used in calculations, is the sum in quadrature of the assigned uncertainties.

Systematic	Assigned uncertainty (%)
Pile up	1
Lepton efficiencies	9
Jet energy resolution	1
Jet energy scale	1
Btagging efficiencies	5
Mistagging efficiencies	1
All combined	11